Supplementary Materials

Programmable Hooded DNA Switches for Conditional Control of CRISPR-Cas12a in Multiplexed Biosensing

Xingyu Zhong[1,†], Xi Gong[1,†], Na Zeng[1,†], Tianci Xie[2], Shaogang Wang[1,] and Qidong Xia[1,*]*

[1] Department and Institute of Urology, Tongji Hospital, Tongji Medical College, Huazhong University of Science and Technology, Wuhan, 430030, China.

[2] GI Cancer Research Institute, Tongji Hospital, Tongji Medical College, Huazhong University of Science and Technology, Wuhan, 430030, China.

† These authors contributed equally to this work.

* To whom correspondence should be addressed: Qidong Xia, E-mail: qidongxia_md@163.com.

Correspondence may also be addressed to Shaogang Wang, E-mail: sgwangtjm@163.com.

1. Supplementary tables

Table S1. Oligonucleotide Sequences Used in Figure 1

Name	Sequence
HAT-Probe	CACATACCCC/i6FAMdT/GGCCGCCCTCTCCA/BHQ1/
HAT	TGGAGAGGGCGTTTTTTTTTTTTTTTTTTTGCCAGGGGTATGTG
HAT-Split-1	TGGAGAGGGCGTTTTTTTTT
HAT-Split-2	TTTTTTTTTGCCAGGGGTATGTG
Ra-1	TGGAGAGGGCGGAAAAATGCGTAGGCGACGTGTAAAAAAAAAATCG ACGTGACGTACG
Ra-2	CGTACGTCACGTCGATTTTTTTTTTACACGTCGCCTACGCATTTTTCCAG GGGTATGTG
Ra-3’-1	TGGAGAGGGCGGAAAAATGCGTAGGCGACGTGTAAAAAAAAAATCGA CGTGACGTACG
Ra-3’-2	CGATTTTTTTTTTACACGTCGCCTACGCATTTTTCCAGGGGTATGTG
Ra-5’-1	TGGAGAGGGCGGGATTTTTTTTTTACACGTCGCCTACGCATTTTTTT
Ra-5’-2	ATGCGCATAAAAAAAAAAATGCGTAGGCGACGTGTAAAAAAAAAATCC CAGGGGTATGTG
CPLT	TGGAGAGGGCGCTGAATTCGGAGTTTTTTTTTTCTCCGAATTCAGGCCA GGGGTATGTG
Probe-Comple ment	TGGAGAGGGCGGCCAGGGGTATGTG
Hairpin	TGGAGAGGGCGGCCAGGGGTATGTGTTTTTTTTTTTTTTTTTTTTTTTTC ACATACCCCTGGCCGCCCTCTCCA
HAT-5T	TGGAGAGGGCGTTTTTGCCAGGGGTATGTG
HAT-6T	TGGAGAGGGCGTTTTTTGCCAGGGGTATGTG
HAT-7T	TGGAGAGGGCGTTTTTTTGCCAGGGGTATGTG
HAT-8T	TGGAGAGGGCGTTTTTTTTGCCAGGGGTATGTG
HAT-9T	TGGAGAGGGCGTTTTTTTTTGCCAGGGGTATGTG

HAT-10T	TGGAGAGGGCGTTTTTTTTTTGCCAGGGGTATGTG
HAT-11T	TGGAGAGGGCGTTTTTTTTTTTGCCAGGGGTATGTG
HAT-12T	TGGAGAGGGCGTTTTTTTTTTTTGCCAGGGGTATGTG
HAT-13T	TGGAGAGGGCGTTTTTTTTTTTTTGCCAGGGGTATGTG
HAT-14T	TGGAGAGGGCGTTTTTTTTTTTTTTGCCAGGGGTATGTG
HAT-15T	TGGAGAGGGCGTTTTTTTTTTTTTTTGCCAGGGGTATGTG
HAT-16T	TGGAGAGGGCGTTTTTTTTTTTTTTTTGCCAGGGGTATGTG
HAT-17T	TGGAGAGGGCGTTTTTTTTTTTTTTTTTGCCAGGGGTATGTG
HAT-18T	TGGAGAGGGCGTTTTTTTTTTTTTTTTTTGCCAGGGGTATGTG
HAT-19T	TGGAGAGGGCGTTTTTTTTTTTTTTTTTTTGCCAGGGGTATGTG
HAT-20T	TGGAGAGGGCGTTTTTTTTTTTTTTTTTTTTGCCAGGGGTATGTG
HAT-21T	TGGAGAGGGCGTTTTTTTTTTTTTTTTTTTTTGCCAGGGGTATGTG
HAT-22T	TGGAGAGGGCGTTTTTTTTTTTTTTTTTTTTTTGCCAGGGGTATGTG
HAT-23T	TGGAGAGGGCGTTTTTTTTTTTTTTTTTTTTTTTGCCAGGGGTATGTG
HAT-24T	TGGAGAGGGCGTTTTTTTTTTTTTTTTTTTTTTTTGCCAGGGGTATGTG
HAT-25T	TGGAGAGGGCGTTTTTTTTTTTTTTTTTTTTTTTTTGCCAGGGGTATGTG
HAT-26T	TGGAGAGGGCGTTTTTTTTTTTTTTTTTTTTTTTTTTGCCAGGGGTATGTG
HAT-27T	TGGAGAGGGCGTTTTTTTTTTTTTTTTTTTTTTTTTTTGCCAGGGGTATGTG
HAT-28T	TGGAGAGGGCGTTTTTTTTTTTTTTTTTTTTTTTTTTTTGCCAGGGGTATGTG
HAT-29T	TGGAGAGGGCGTTTTTTTTTTTTTTTTTTTTTTTTTTTTTGCCAGGGGTATGTG
HAT-30T	TGGAGAGGGCGTTTTTTTTTTTTTTTTTTTTTTTTTTTTTTGCCAGGGGTATGTG
HAT-0-Split-1	TGGAGAGGGCGTTTTTTTTT
HAT-0-Split-2	TTTTTTTTTGCCAGGGGTATGTG
HAT-1-Split-1	TGGAGAGGGCTTTTTTTTT
HAT-1-Split-2	TTTTTTTTTGCCAGGGGTATGTG

HAT-2-Split-1	TGGAGAGGGCTTTTTTTTT
HAT-2-Split-2	TTTTTTTTTCCAGGGGTATGTG
HAT-3-Split-1	TGGAGAGGGTTTTTTTTT
HAT-3-Split-2	TTTTTTTTTCCAGGGGTATGTG
HAT-4-Split-1	TGGAGAGGGTTTTTTTTT
HAT-4-Split-2	TTTTTTTTTCAGGGGTATGTG
HAT-5-Split-1	TGGAGAGGTTTTTTTTT
HAT-5-Split-2	TTTTTTTTTCAGGGGTATGTG
HAT-6-Split-1	TGGAGAGGTTTTTTTTT
HAT-6-Split-2	TTTTTTTTTAGGGGTATGTG
T-shaped DNA-1	TGGAGAGGGCGATCGCTCAGA
T-shaped DNA-2	TCTGAGCGAGCCAGGGGTATGTG
Scaffold RNA	AAUUUCUACUAAGUGUAGAU
Spacer RNA	UUUGUUCGUUCGGCUCGCGUGA
Spacer DNA	TCACGCGAGCCGAACGAACAAA

Table S2. Oligonucleotide Sequences Used in Figure 2

Name	Sequence
Scaffold RNA	AAUUUCUACUAAGUGUAGAU
Hairpin-25nt	/FAM/CACATACCCCTGGCCGCCCTCTCCATTTTTTTTTTTTTTTTTTTTTTTTTGGAGAGGGCGGCCAGGGGTATGTG/BHQ1/
Hairpin-10nt	/FAM/GCCCTCTCCCTTTTTTTTTTTTTTTTTTTTTTTTGGGAGAGGGC/BHQ1/
Hairpin-5nt	/FAM/CTCCCTTTTTTTTTTTTTTTTTTTTTTTTGGGAG/BHQ1/
HAT-Probe	CACATACCCC/i6FAMdT/GGCCGCCCTCTCCA/BHQ1/
HAT-25T	TGGAGAGGGCGTTTTTTTTTTTTTTTTTTTTTTTTGCCAGGGGTATGTG

Table S3. Oligonucleotide Sequences Used in Figure 3 and 4

Name	Sequence
DNAzyme	CATCTCTTCTCCGAGCCGGTCGAAATAGTGAGT
HAT-rA	TGGAGAGGGCGTTTTTTTTTTTTTT/rA/TTTTTTTTTTTTTTGCCA GGGGTATGTG
HAT-Probe	CACATACCCC/i6FAMdT/GGCCGCCCTCTCCA/BHQ1/
DPA	TTTTTTTTAATTAAAGCTCGCCATCAAATAGCTTTTTTTTTTGCTA TTTGATGGCGATCCGAGCCGGTCGAATAGGAGATCG
DPA-Probe	CGATCTCCTAT/rA/GTCGCCA
HAT-Probe-@AuNPs	/FAM/CACATACCCCGGCCGCCCTCTCCA/C6 SH-SH/

Table S4. Oligonucleotide Sequences Used in Figure 5

Name	Sequence
miR-375-3p-F	AACCGGTTTGTTCGTTCGGCT
miR-375-3p-R	ATCCAGTGCAGGGTCCGAGG
miR-375-3p-sl	GTCGTATCCAGTGCAGGGTCCGAGGTATTCGCACTGGATACGACTCACGC
miR-21-5p-F	GCGCGTAGCTTATCAGACTGA
miR-21-5p-R	ATCCAGTGCAGGGTCCGAGG
miR-21-5p-sl	GTCGTATCCAGTGCAGGGTCCGAGGTATTCGCACTGGATACGACTCAACA
miR-141-3p-F	GAGCGCGTAACACTGTCTGGTA
miR-141-3p-R	ATCCAGTGCAGGGTCCGAGG
miR-141-3p-sl	GTCGTATCCAGTGCAGGGTCCGAGGTATTCGCACTGGATACGACCCCATCT
hsa-miR-148a-3p_sl	GGAGAGGAGAGGAAGAGGGAAATCTCCTCTCCACAAAG
hsa-miR-148a-3p_F	GGGTCAGTGCACTACAGAA
hsa-miR-148a-3p_R	GAGAGGAGAGGAAGAGGGAA
hsa-miR-342-3p_sl	GCTCCTCCTATCCTCCTCGTCATAGGAGGAGCACGGGT
hsa-miR-342-3p_F	GGGTCTCACACAGAAATCGC
hsa-miR-342-3p_R	CTCCTCCTATCCTCCTCGTC

Table S5. Oligonucleotide Sequences Used in Figure 6

Name	Sequence
S1	ACATTCCGTCTGAAACATTACATGCTACACGAGAAGAGCCATAGTATTTTT TACCTGGGGGAGTATTGCGGAGGAAGGT
S2	TATCACCCAGTTGACAGTGTAGCATGTAATAGATGCGAGCCAATACTTTTTT ACCTGGGGGAGTATTGCGGAGGAAGGT
S3	TCAACTGGGTGATAAAACGACACTTGGGAATCTACTATGGCTCTTCTTTTTT ACCTGGGGGAGTATTGCGGAGGAAGGT
S4	TTCAGACGGAATGTGCTTCCCAAGTGTCGTTTGTATTGGCTCGCATTTTTTT ACCTGGGGGAGTATTGCGGAGGAAGGT
S1-linker	ACATTCCGTCTGAAACATTACATGCTACACGAGAAGAGCCATAGTATTTTT TACCTGGGGGAGTATTGCGGAGGAAGGT
S2-linker	TATCACCCAGTTGACAGTGTAGCATGTAATAGATGCGAGCCAATACTTTTTT ACCTGGGGGAGTATTGCGGAGGAAGGT
S3-linker	TCAACTGGGTGATAAAACGACACTTGGGAATCTACTATGGCTCTTCTTTTTT ACCTGGGGGAGTATTGCGGAGGAAGGT
S4-linker	TTCAGACGGAATGTGCTTCCCAAGTGTCGTTTGTATTGGCTCGCATTTTTTT ACCTGGGGGAGTATTGCGGAGGAAGGT
HAT-UD G-PROBE	T*G*G*A*G*A*G*G*G*C*G*T*T*T*T*T*T*T*T*T*T*T*T*T*T*T*T*T*T*T*T*T*T*G *C*C*A*G*G*G*G*/dU/*A*T*G*T*G

*-Phosphorothioate

Table S6. Oligonucleotide Sequences Used in Figure S5

Name	Sequence
Scaffold RNA	AAUUUCUACUAAGUGUAGAU
MiR-375	UUUGUUCGUUCGGCUCGCGUGA
DNA-375	TCACGCGAGCCGAACGAACAAA
MiR-21	UAGCUUAUCAGACUGAUGUUGA
DNA-21	TCAACATCAGTCTGATAAGCTA
MiR-141	UAACACUGUCUGGUAAAGAUGG
DNA-141	CCATCTTTACCAGACAGTGTTA
MiR-7	CAACAAAUCACAGUCUGCCAUA
DNA-7	TATGGCAGACTGTGATTTGTTG
MiR-148	UCAGUGCACUACAGAACUUUGU
DNA-148	ACAAAGUUCUGUAGUGCACUGA
MiR-296	GAGGGUUGGGUGGAGGCUCUCC
DNA-296	GGAGAGCCUCCACCCAACCCUC
MiR-342	UCUCACACAGAAAUCGCACCCGU
DNA-342	ACGGGUGCGAUUUCUGUGUGAGA

2. Supplementary Figures

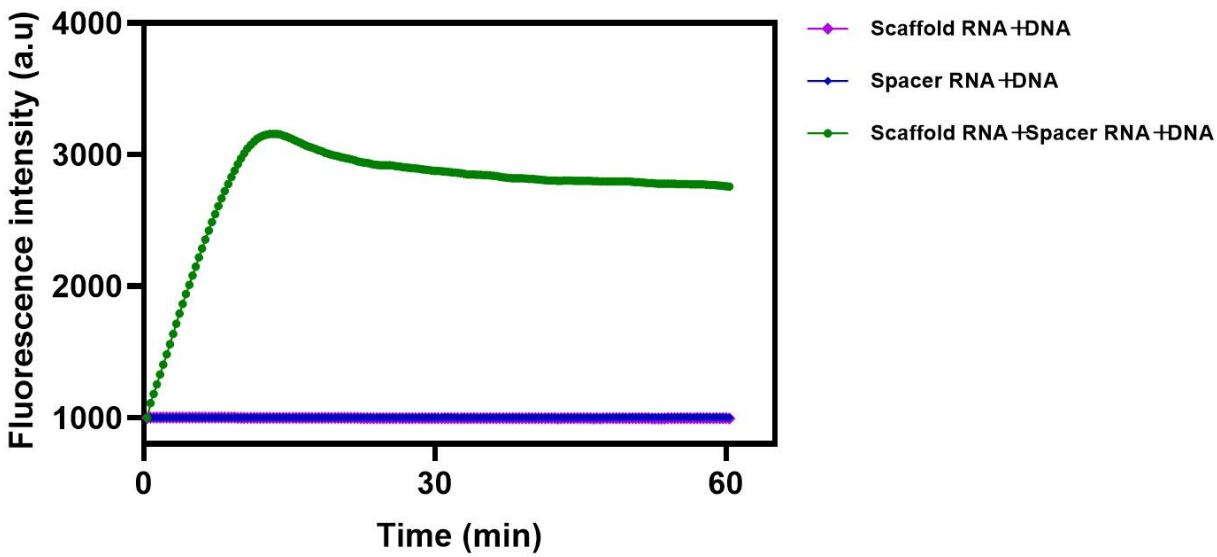

Figure S1. The working principle of the split CRISPR/Cas12a assay: Cas12a is activated to produce fluorescence exclusively when both the scaffold RNA and the target DNA are present concurrently.

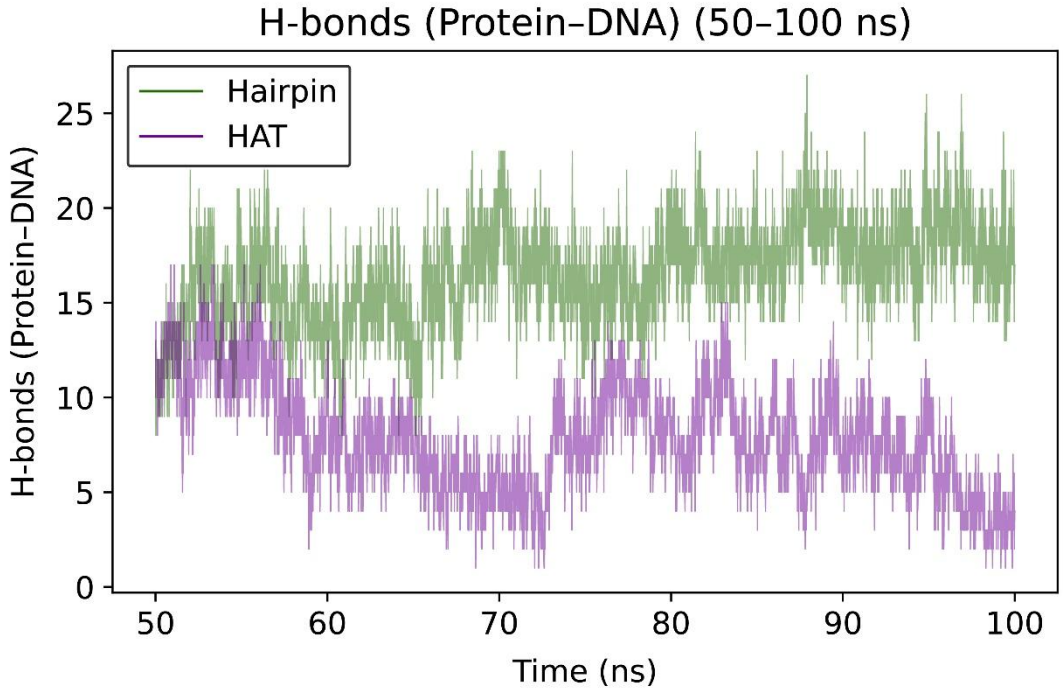

Figure S2. Number of hydrogen bonds formed between Cas12a and the DNA reporters during the stable simulation window.

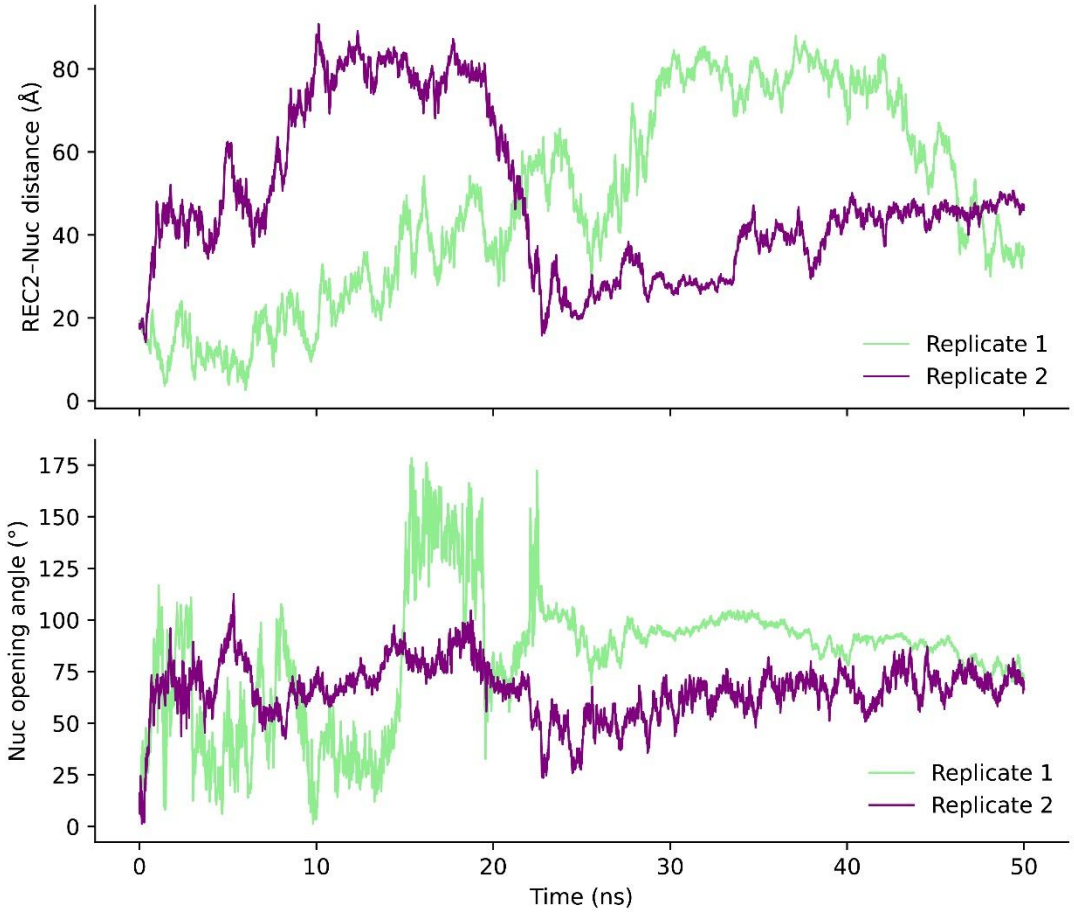

Figure S3. Minimum distance between Cas12a and the HAT (or Hairpin) DNA reporters during MD simulations, showing no significant difference between the two complexes.

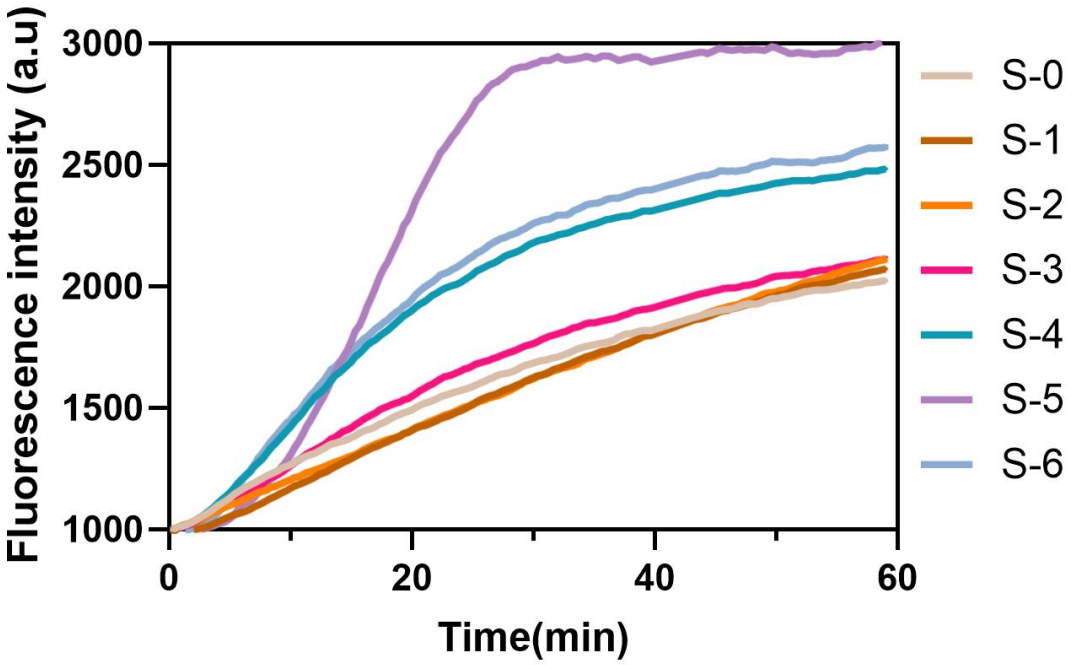

Figure S4. Fluorescence curve analysis of cap-opening size control in HAT-structured probes after separation, Labels S-0 through S-6 correspond to cap-opening sizes ranging from 0 bp to 6 bp.

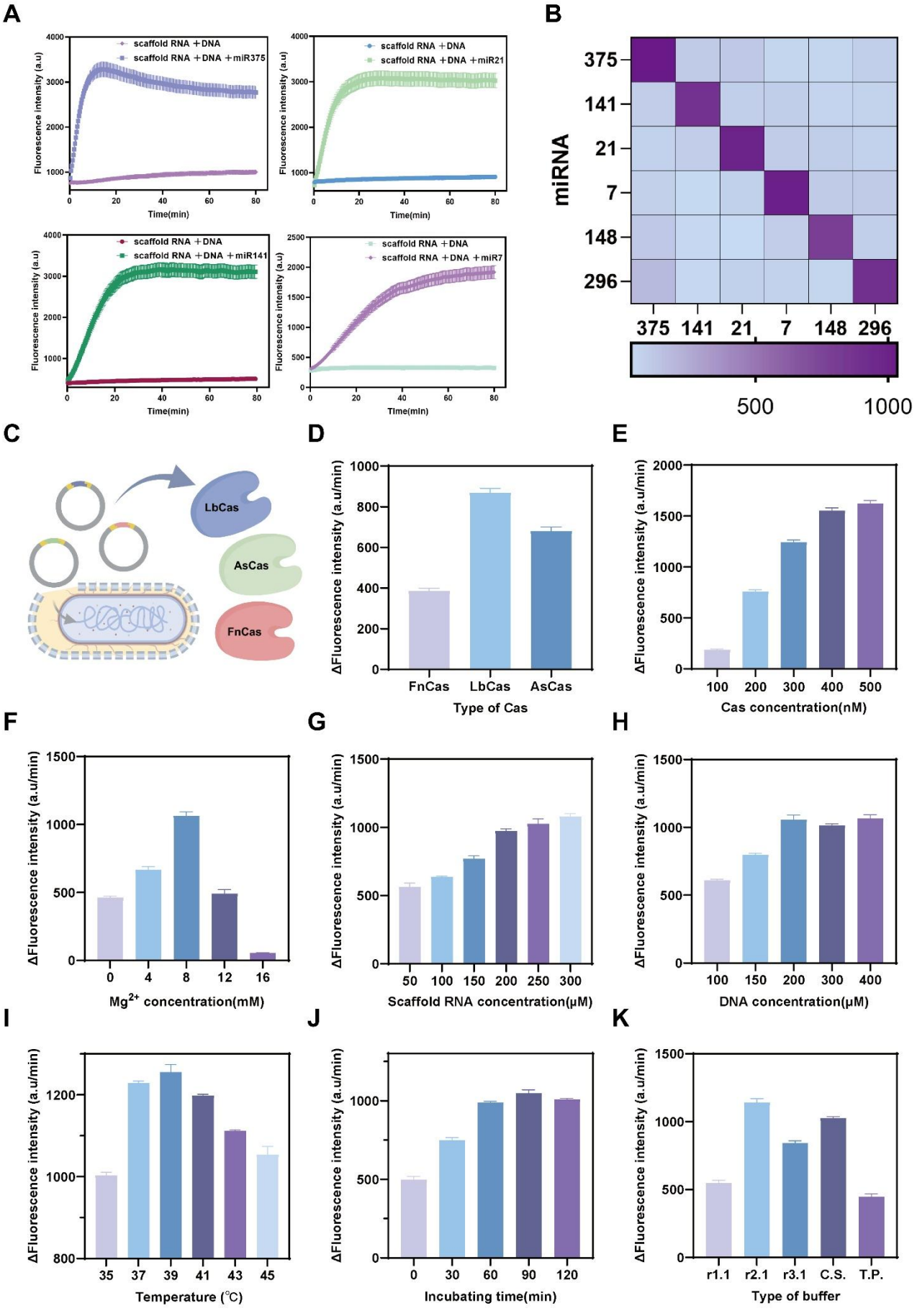
A
scaffold RNA +DNA
scaffold RNA +DNA +miR375
scaffold RNA +DNA +miR21
scaffold RNA +DNA +miR141
scaffold RNA +DNA +miR7
Fluorescence intensity (a.u)
Time(min)
B
miRNA
375
141
21
7
148
296
500
1000
C
LbCas
AsCas
FnCas
D
ΔFluorescence intensity (a.u/min)
FnCas
LbCas
AsCas
Type of Cas
E
Cas concentration(nM)
F
Mg2+ concentration(mM)
G
Scaffold RNA concentration(μM)
H
DNA concentration(μM)
I
Temperature (℃)
J
Incubating time(min)
K
r1.1
r2.1
r3.1
C.S.
T.P.
Type of buffer

Figure S5. Characterization and optimization of Split CRISPR/Cas12a system. (A-B) Validation of the CRISPR/Cas12a system for miRNA cleavage and its specificity. (A) Cleavage of miR-375, miR-21, miR-141, and miR-7 by CRISPR/Cas12a. (B) Specificity of CRISPR/Cas12a-mediated cleavage across different miRNA.(C-D) Production and activity comparison of different Cas proteins. (C) Schematic diagram of the production processes for FnCas12a, LbCas12a, and AsCas12a. (D) Comparison of the enzymatic activities of the three Cas12a proteins. (E-H) System performance evaluation under varying concentrations of: (E) Cas12a protein, (F) Mg^{2+} ions, (G) scaffold RNA, and (H) target DNA, as measured by fluorescence intensity. (I-K) Optimization parameters: (I) Reaction temperature, (J) incubation duration, and (K) buffer composition (C.S.: CutSmart; T.P.: ThermoPol), assessed through fluorescence intensity measurement.

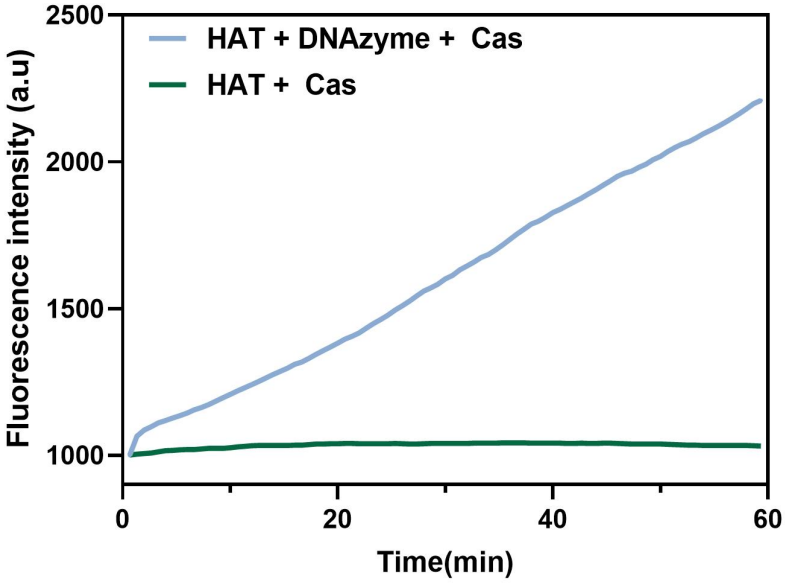

Figure S6. Investigation of cleavage activity of standalone DNAzyme on rA-modified HAT duplex.

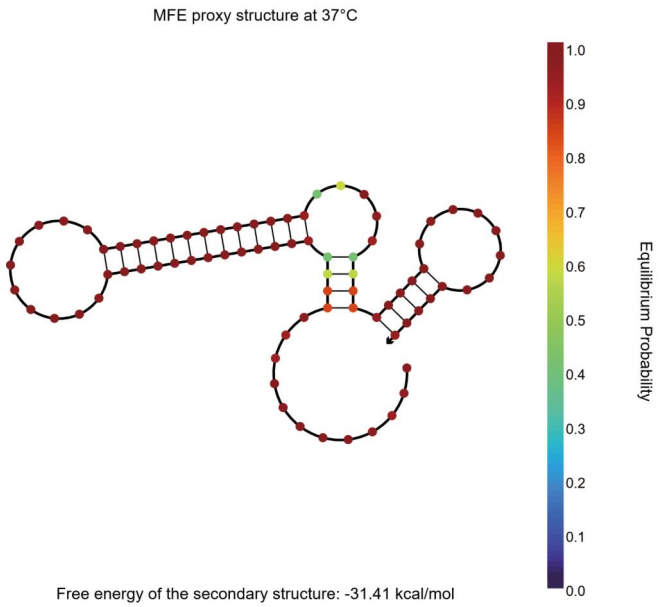

Figure S7. In silico structure prediction of the DPA construct by NUPACK software.

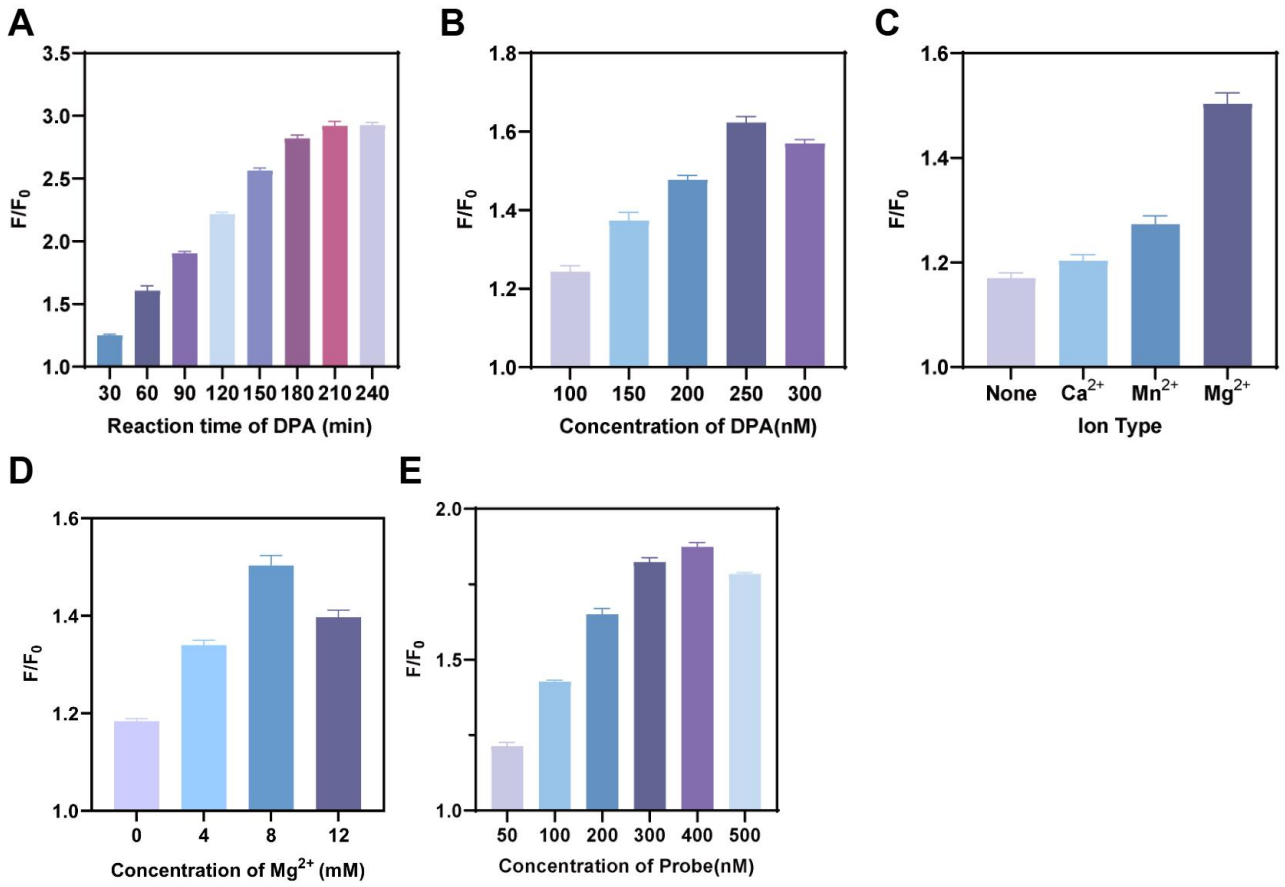

Figure S8. Optimization of reaction conditions including reaction time of DPA (A), concentration of DPA (B), ion type (C), concentration of Mg^{2+} (D) and concentration of the probe (E).

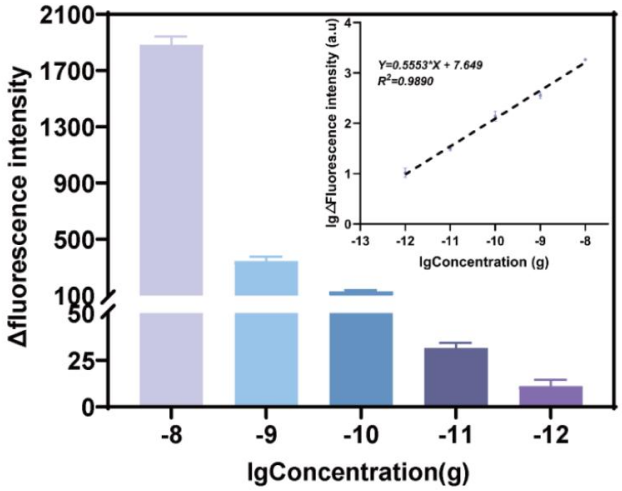

Figure S9. The fluorescence signal output by DPA is linearly correlated with the logarithm of PSA concentration.

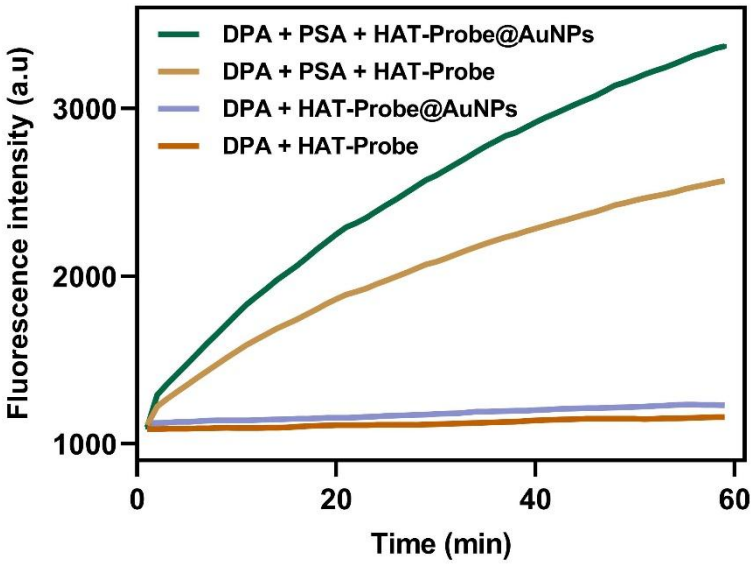

Figure S10. The enrichment effect of AuNPs can improve the sensitivity of detection systems.

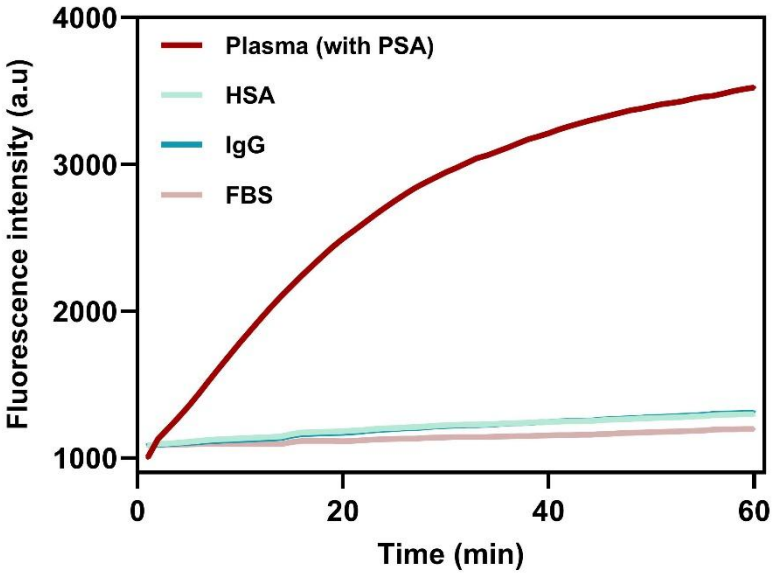

Figure S11. The ability of SCHP system to distinguish irrelevant interfering proteins.

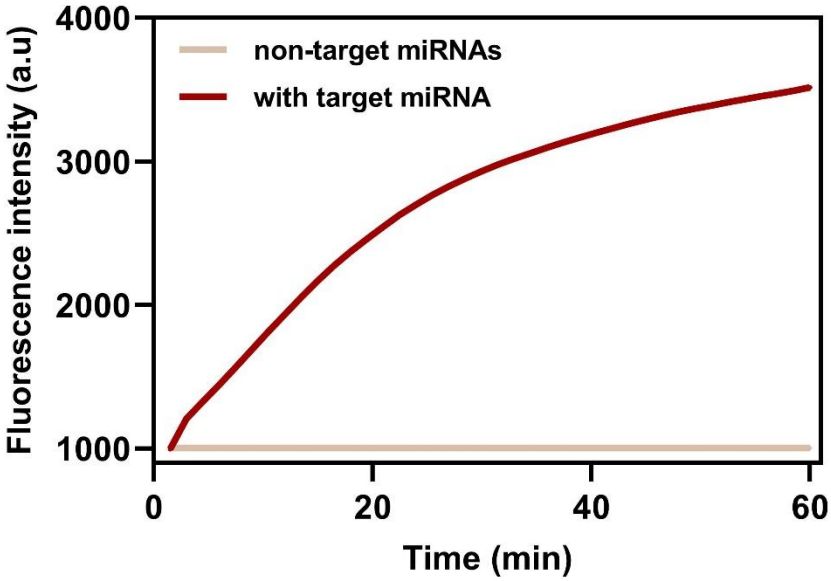

Figure S12. The ability of dual-mode detection system to distinguish interfering miRNAs.

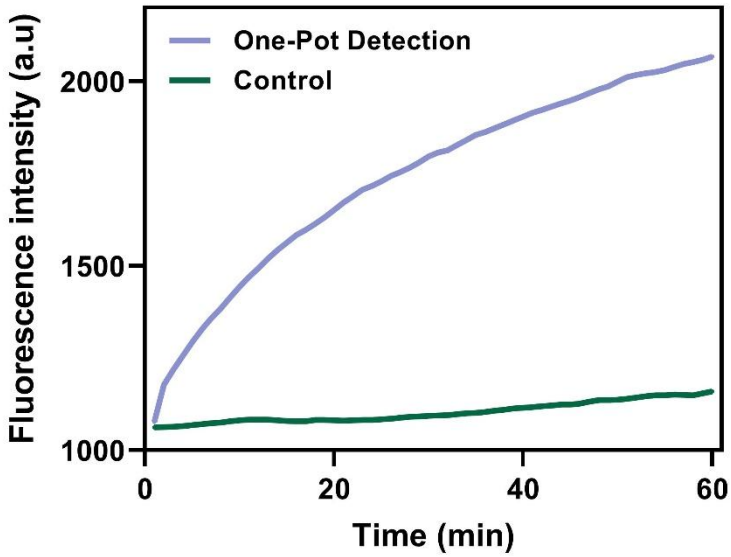

Figure S13. One-Pot Detection method was used to detect PSA and miRNA based on SHDP system. To a 200 μL PCR tube, add 2uL DPA (5uM), 2ng PSA, 5uL HAT-Probe@AuNP (2uM), 2uL scaffold RNA (5uM), 2uL spacer RNA (5uM), 2uL DNA (5uM), 4uL Mg^{2+} (100 mM), 1 uL LbCas12a protein (10 uM), 5 μL buffer r2.1 (10×) and brought up to a total volume of 50 μL by DEPC water. Incubate at 39 °C while monitoring the fluorescence intensity in real time.

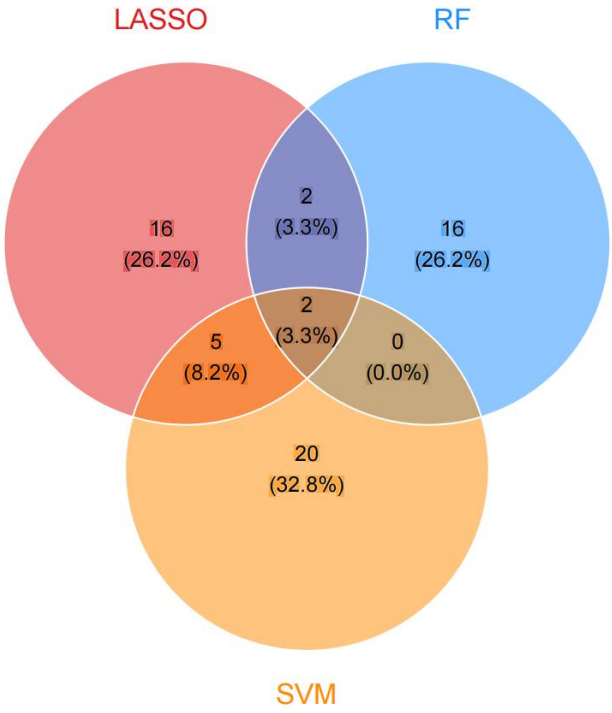

Figure S14. Venn graph from the selected genes (from TCGA).

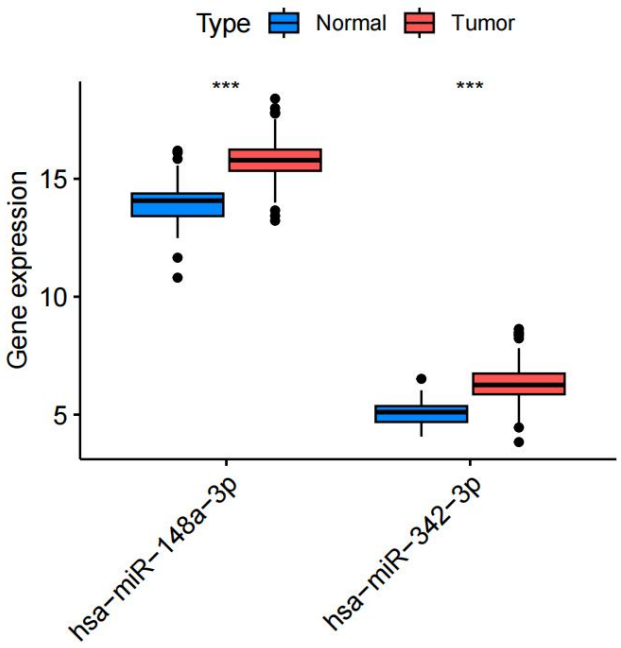

Figure S15. Comparison of expression levels of hsa-miR-148a-3p and hsa-miR-342a-3p in tumor versus normal tissues (data from TCGA).

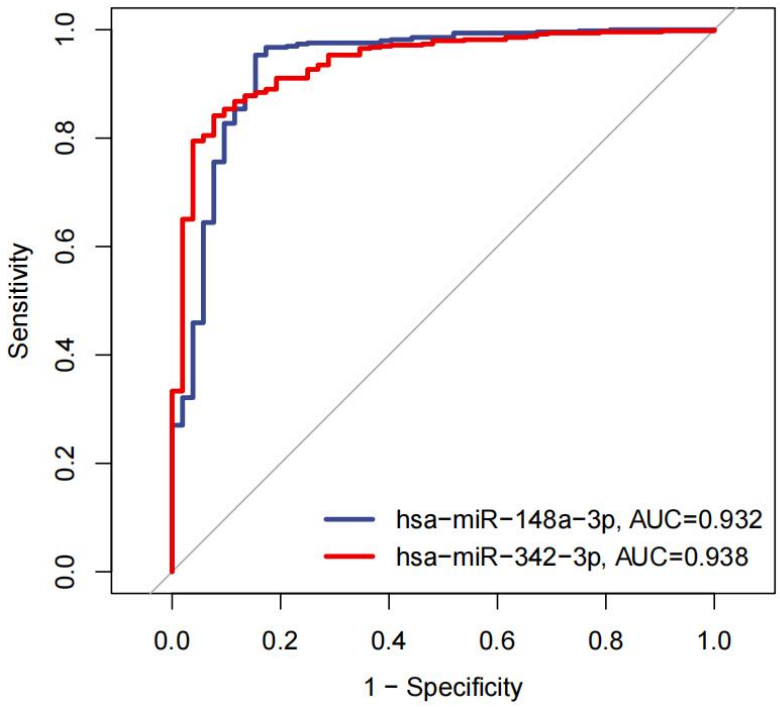

Figure S16. ROC curves for predicting prostate cancer (PCa) using hsa-miR-148a-3p and hsa-miR-342a-3p (data from TCGA).

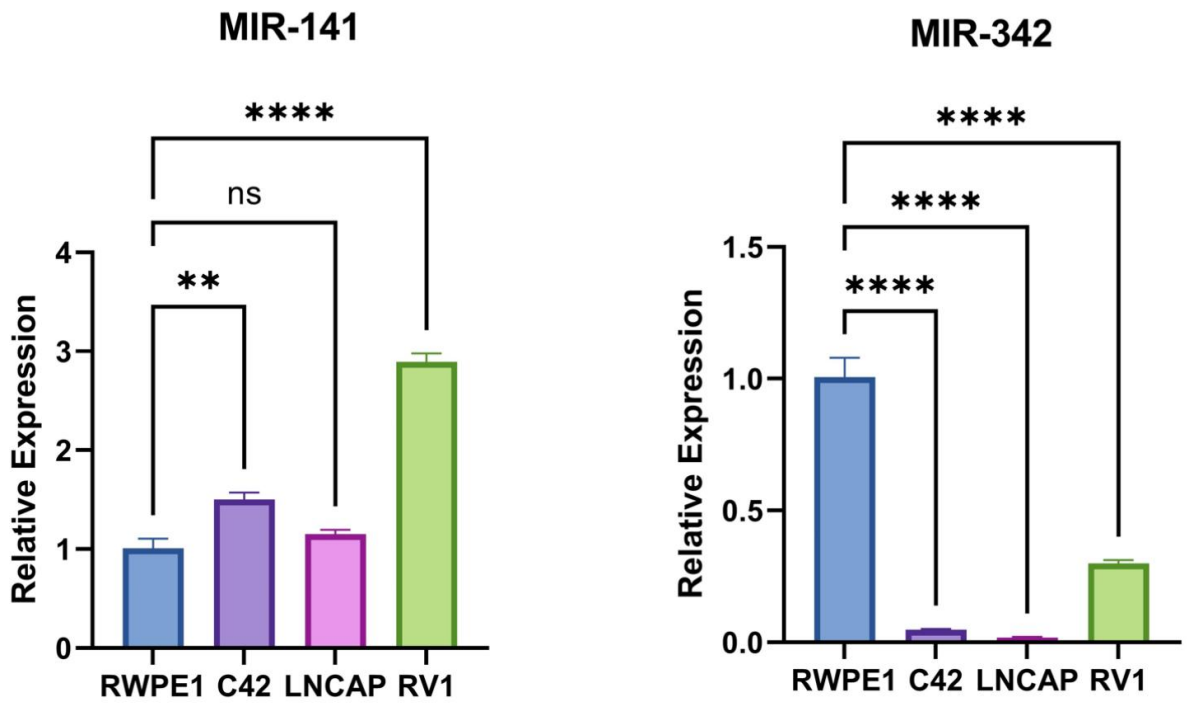

Figure S17. Analysis of miR-141 and miR-342 expression in prostate epithelial cells and prostate cancer cell lines by RT-qPCR. These miRNAs were excluded from further study because miR-141 showed no consistent significant differential expression, and miR-342 exhibited a trend opposite to that observed in the TCGA data.

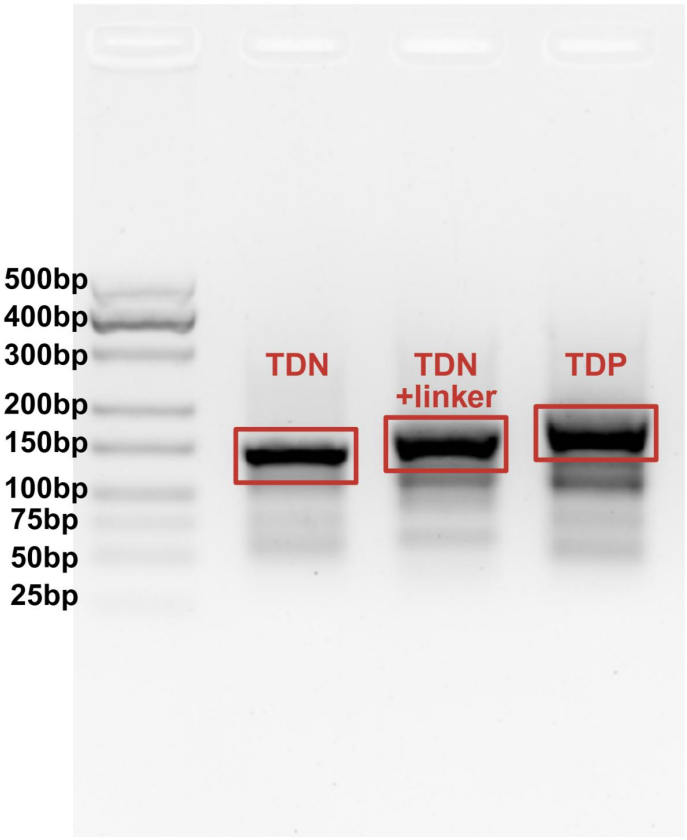

Figure S18. The assembly of Tetrahedral DNA Nanostructure (TDN), TDN with linker (TDN functionalized with linker but without probe), and TDP (Tetrahedral DNA Plus Probe) was analyzed using gel electrophoresis.

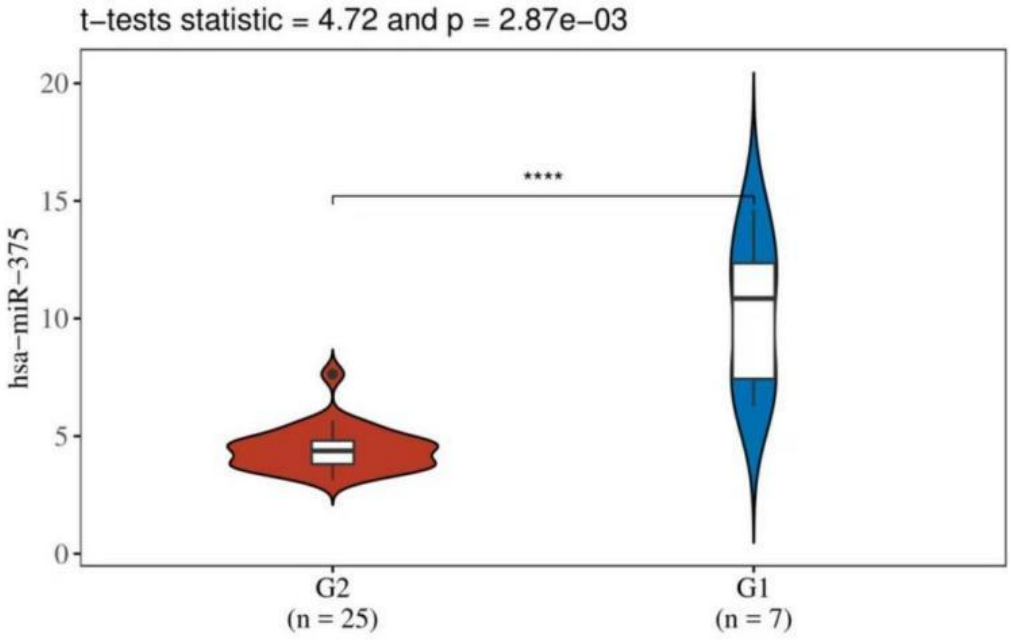

Figure S19. Differential expression of miR-375 between G1 (normal urothelial cells) and G2 (bladder cancer cell lines) based on the CCLE database.

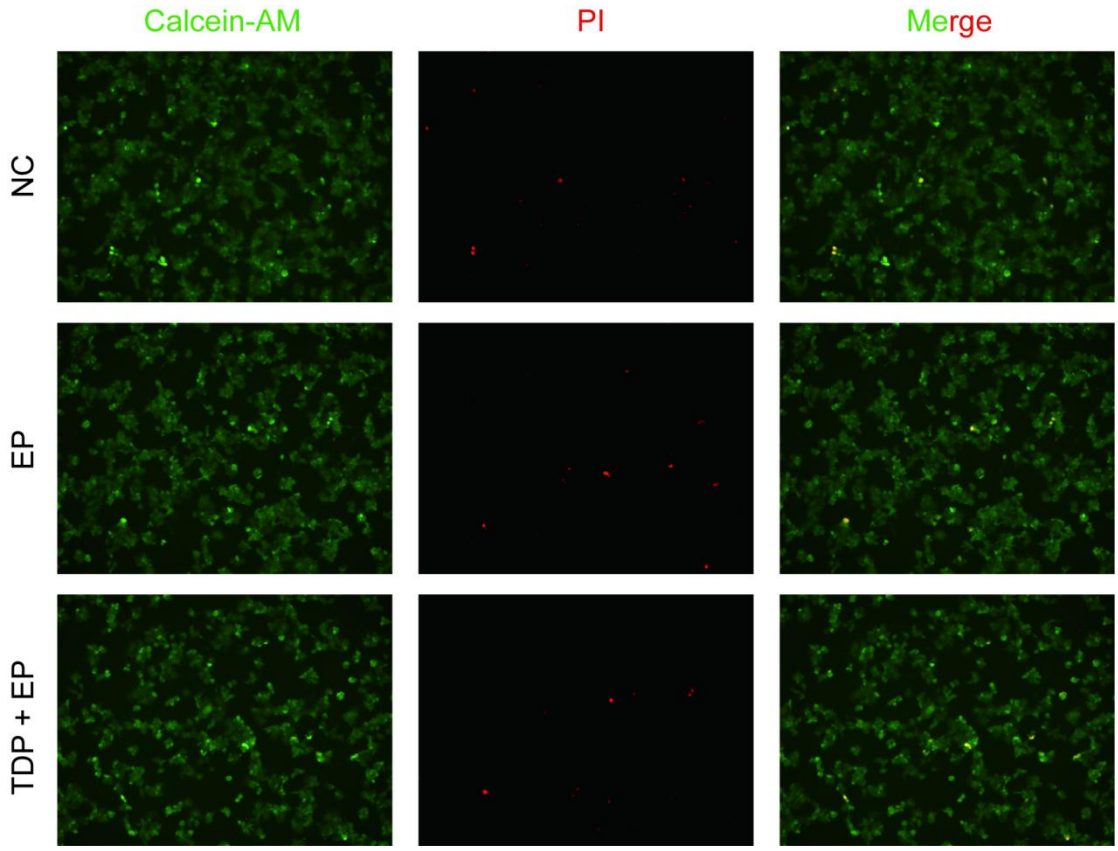

Figure S20. Fluorescence-based viability staining of cells death detection before and after electroporation. (NC: Negative Control, EP: electroporation).